SLAC-PUB-8885
June 2001

New Simulation Results for the Electron-Cloud Effect at the PEP-II Positron Ring*

Y. Cai, S. Heifets, and J. Seeman
Stanford Linear Accelerator Center, Stanford University,
Stanford, CA 94309
M. Furman and M. Pivi
Lawrence Berkeley National Laboratory,
Berkeley, CA 94720

Abstract

We present simulation results for the emittance blowup due to the head-tail effect induced by the electron-cloud effect (ECE) in the low-energy ring (LER) at the PEP-II B factory at SLAC.

(talk presented at the 2001 Particle Accelerator Conference, June 18-22, 2001, Chicago, Illinois.)

*Work supported by the Department of Energy under Contract No. DE-AC03-76SF00515 and DE-AC03-76SF00098.

NEW SIMULATION RESULTS FOR THE ELECTRON-CLOUD EFFECT AT THE PEP-II POSITRON RING*

Y. Cai, S. Heifets and J. Seeman, SLAC, Stanford, CA 94309, USA
M. Furman and M. Pivi, LBNL, Berkeley, CA 94720, USA

Abstract

We present simulation results for the emittance blowup due to the head-tail effect induced by the electron-cloud effect (ECE) in the low-energy ring (LER) at the PEP-II B factory at SLAC.

1 INTRODUCTION

The ECE has been observed or is expected at many storage rings [1, 2]. In particular, there is strong evidence for it in the PEP-II positron ring, where it has led to localized vacuum pressure rises and an emittance blowup that has a strong bunch-to-bunch dependence along the bunch train.

In this article we present an attempt to explain the emittance blowup by means of simulations. These simulations are carried out in two separate stages: in the first, we estimate the electron-cloud density for a given fill pattern. In the second, we take the density thus obtained and feed it as an input parameter into a second simulation that computes the beam blowup. The first simulation is done for rigid, nondynamical bunches with a code that has been under development at LBNL for some time [3, 4]. In the second simulation, the electron cloud is assumed static, and the bunches dynamical. This second part is done with a new code developed at SLAC, described below, using a simple simulation model introduced by Ohmi and Zimmermann [5].

2 ELECTRON CLOUD

We consider only the main two sources of electrons, namely: (1) photoelectrons arising from the synchrotron radiation hitting the walls of the vacuum chamber, and (2) secondary emission from electrons hitting the walls. The model used for the secondary emission yield (SEY) of the TiN-coated chamber is described elsewhere [3, 4]; we have slightly updated it, however, by fitting its parameters to newer measurements obtained at SLAC, both of the SEY and the emitted-electron energy spectrum [6], of TiN-coated aluminum samples of the PEP-II LER vacuum chamber.

We assume a fill pattern whose basic bunch spacing is 4 RF buckets, and has 8 gaps along the circumference, as shown in Fig. 1. Figure 2 shows the simulated density of the electron cloud for the case of $N_b = 5 \times 10^{10}$ positrons per bunch, assuming an effective quantum efficiency per penetrated photon $Y' = 1$. Here we only count those electrons within 5 mm of the beam axis, since it is only these that contribute significantly to the emittance blowup.

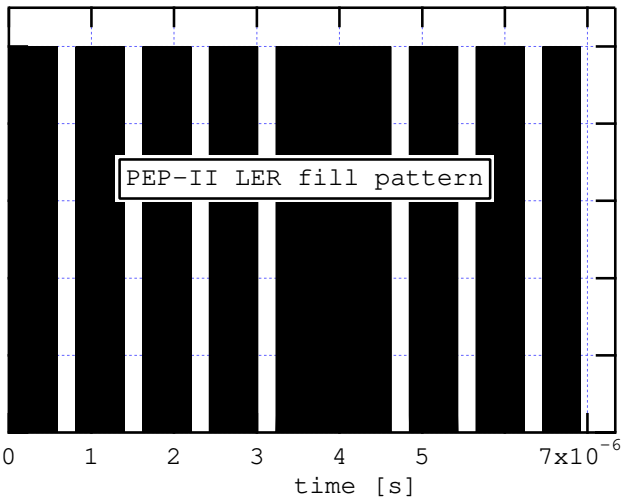

Figure 1: Fill pattern used for the simulation (one full revolution).

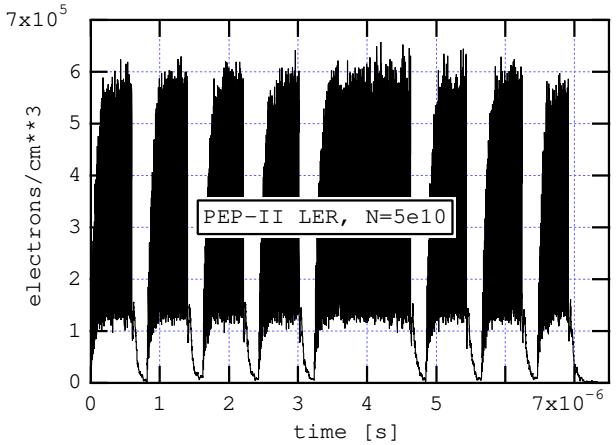

Figure 2: Density of the electron cloud along the bunch train inside a circle of radius 5 mm about the center of the chamber.

*Work supported by the US DOE under contracts no. DE-AC03-76SF00515 and DE-AC03-76SF00098.

3 EMITTANCE BLOWUP

An object-oriented C++ class library has been written to simulate the interaction between the electron cloud and positron beam. In the library, the electron cloud and positron beam are independent objects that can be constructed by the user. There is no limitation on how many objects of cloud are allowed in the simulation, and the clouds can have different parameters as instances of the cloud class. These features provide us with great flexibility to study various phenomena of the ECE.

We represent the transverse distribution of the electron cloud by N_m macroparticles at a given location s in the ring,

$$f_{\perp}^{-}(\vec{x}_e, \vec{v}_e; s) = \frac{1}{N_m} \sum_{n=1}^{N_m} \delta(\vec{x}_e - \vec{x_{e}}_n(s)) \delta(\vec{v}_e - \vec{v_{e}}_n(s)), \tag{1}$$

where $\vec{x}_e$ and $\vec{v}_e$ represent the transverse coordinate and velocity of the electrons. The distribution of the positron bunch is represented by N_s longitudinal macro slices. All slices are assumed to have a rigid Gaussian distribution of transverse rms sizes (σ_x, σ_y). The centroid of each slice is treated as a dynamical variable in 6D phase space.

Transversely, we use the 2D vectors $\vec{x}_c$ and $\vec{p}_c$ to describe the centroid coordinate and canonical momentum of the slices. At the beginning of the simulation, all the transverse coordinates and momenta of the slice centroids are set to zero. Longitudinally, the centroid coordinate z and momentum p_z of the slices are initialized to a Gaussian distribution with rms bunch length σ_z and energy spread σ_p, respectively.

To speed up the simulation, all electrons are lumped into one single slice at a given azimuthal location s with average β function. This approximation is justified because we know that the head-tail instability is rather insensitive to the location of the impedance. Before the arrival of the positron bunch, the distribution of electron cloud is reinitialized to a Gaussian distribution with sizes σ_x^c and σ_y^c and the velocities of the electrons are reset to zero. The slices of the bunch are sorted according to their longitudinal position. Starting with the head, the slices collide with the electron cloud sequentially in time. Under the assumption of Gaussian distribution, the kick experienced by i^{th} electron from the electric field of n^{th} slice is

$$\delta\vec{v_{e}}_i = -\frac{2N_b r_e c}{N_s} \vec{F_G}(\vec{x_{e}}_i - \vec{x_{c}}_n; \vec{\sigma}), \tag{2}$$

where $\vec{F_G}$ is given by the Erskine-Bassetti formula [7]. The kick by the electron cloud to the centroid of the slice is expressed as

$$\delta\vec{p_{c}}_n = -\frac{2r_e N_e}{N_m \gamma} \sum_{i=1}^{N_m} \vec{F_G}(\vec{x_{c}}_n - \vec{x_{e}}_i; \vec{\sigma}), \tag{3}$$

where $N_e = 2\pi\sigma_x^c\sigma_y^c C n_e$. Note that the distribution of the electron cloud is not directly used in the calculation and the expression is based on the conservation of the momentum. Because the transverse size of the electron cloud is much larger than that of the beam, the approximation is adequate. Between the collision of two adjacent slices the electrons drift, $\delta\vec{x_e} = \vec{v_e} dz/c$, where dz is the slice separation.

To see the dynamical effects of the positron beam, we track the centroid of the slices with betatron and synchrotron motions. The transverse coordinates are tracked by applying a simple linear Courant-Snyder map around the ring with tunes ν_x and ν_y and lattice functions β_x, α_x, etc. In the longitudinal plane similar formulas are applied, with $\beta_z = \sigma_z/\sigma_p$ and $\alpha_z = 0$.

Current operating parameters of the LER are listed in Table 1. All wiggler magnets in the machine are turned off for higher luminosity. The vertical emittance is estimated from the beam-beam luminosity scan. The average of the beta function is computed using the values at the end of every element. The bunch charge N_b is chosen to correspond to the highest operating current in the ring.

Table 1: Parameters for the LER.

Parameter	Description	Value
E [Gev]	beam energy	3.1
β_x [m]	average x beta	9.370
β_y [m]	average y beta	12.47
ϵ_x [nm-rad]	x emittance	24.0
ϵ_y [nm-rad]	y emittance	1.50
σ_z [cm]	rms bunch length	1.30
σ_p	relative energy spread	7.7×10^{-4}
ν_x	x tune	0.649
ν_y	y tune	0.564
ν_s	synchrotron tune	0.0251
C [m]	circumference	2200
N_b	positrons/bunch	1×10^{11}
α	momentum compaction	1.23×10^{-3}

The other parameters used in the simulations are listed in Table 2. The parameters related to the electron cloud are not yet well established. In Fig. 2 we see that the saturation density is $n_e \simeq 6 \times 10^5$ cm^{-3} for $N_b = 5 \times 10^{10}$. Other simulations show that n_e is higher at higher N_b, but we do not yet have a reliable estimate. The number of slices in the bunch and macro particles for the electron cloud is balanced between a better accuracy and computational time. They are limited by the requirement of 24 hours turnaround time on a computer workstation. These parameters are always used in the simulation unless statements to the contrary in the text.

4 RESULTS AND DISCUSSION

Based on the analytical derivation of the wake field generated by the electron cloud and the theory of instability in the previous section, it is clear that there is a threshold of strong head-tail instability ($\xi_x = \xi_y = 0$). In this section

Table 2: Simulation parameters.

Parameter	Description	Value
n_e [cm^{-3}]	e-cloud density	8.0×10^5
σ_x^c [mm]	e-cloud x size	6.0
σ_y^c [mm]	e-cloud y size	3.0
N_s	no. of slices	1024
N_m	no. of macro particles	10240

we simulate the interaction between the electron cloud and the positron beam and the beam dynamics to compare the result with the analytical approximation. We vary the intensity of the electron cloud n_e from 1×10^5 to 1×10^6 cm^{-3} and find that the vertical instability approximately occurs at 5×10^5 cm^{-3} as shown in Fig. 3. The turn-by-turn evolution of the rms value of slices is plotted in the figure. One can see that, beyond the threshold, the centroids of the slices spread widely comparing to the beam size, leading to an effective increase of the emittance of the beam. To quantify the emittance growth, we define $\Sigma_y = (\sigma_y^2 + \sigma_{c,y}^2)^{1/2}$, where $\sigma_{c,y}$ is the vertical rms variation of the centroid, and plot it as a function of the cloud density in the second plot. Σ_y can be measured with a synchrotron light monitor.

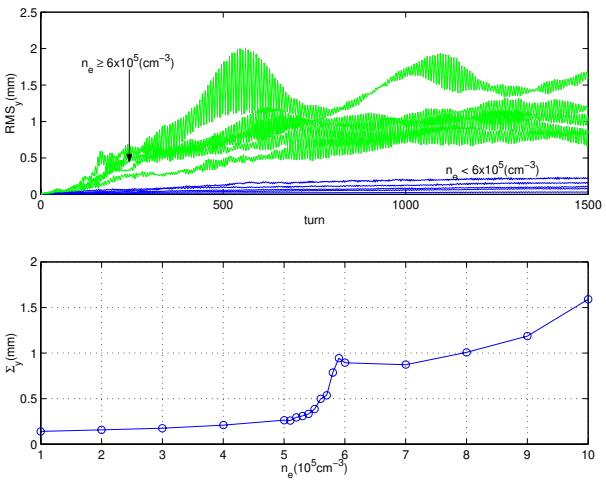

Figure 3: Threshold of head-tail instability caused by electron cloud.

It is well known that the lattice chromaticities can play an important role to stabilize the conventional head-tail instability. To study this effect, we vary ξ_y in the range $-10 < \xi_y < 10$ while fixing $\xi_x = 0$ and $n_e = 8 \times 10^5$ cm^{-3}, which is above the instability threshold. The results are shown in Fig. 4. One can see that $\xi_y < 0$ leads to large beam blowup while $\xi_x > 0$ does not, in agreement with experimental observations.

In conclusion, we see clear threshold behaviors of beam blowup as a function of electron cloud density and chromaticity. The actual value of the electron cloud density remains to be better determined. A clear signal of bunch-to-bunch variation of the electron density along the train, if it exists, will require further simulations with much better statistics.

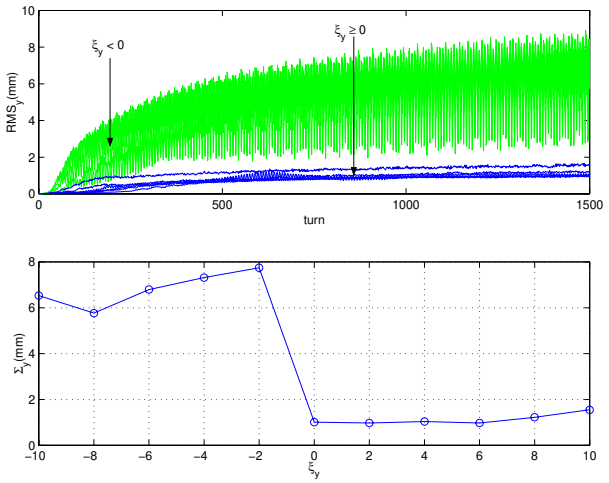

Figure 4: Effective beam size as a function of chromaticity.

5 ACKNOWLEDGMENTS

We are grateful to R. Kirby for discussions on the SEY, and to NERSC for supercomputer support.

6 REFERENCES

[1] For a summary, see Proc. ICFA Workshop on Two-Stream Instabilities, Santa Fe, NM, Feb. 16–18, 2000, http://www.aps.anl.gov/conferences/icfa/two-stream.html

[2] G. Rumolo, F. Ruggiero and F. Zimmermann, PRST-AB **4**, 012801 (2001) (erratum: **4**, 029901 (2001)). See also F. Zimmermann, these proceedings.

[3] M. A. Furman and G. R. Lambertson, Proc. Intl. Workshop on Multibunch Instabilities in Future Electron and Positron Accelerators (MBI-97), KEK, Tsukuba, Japan, 15-18 July 1997 (KEK Proceedings 97-17, Dec. 1997, p. 170); http://www.lbl.gov/~miguel/MBI97-ECI-PEPII.pdf

[4] M. A. Furman, LBNL-41482/CBP Note 247/LHC Project Report 180, May 20, 1998, http://www.lbl.gov/~miguel/LHCpr180.pdf

[5] K. Ohmi and F. Zimmermann, Phys. Rev. Lett. **85** 3821 (2000).

[6] R. E. Kirby and F. K. King, SLAC-PUB-8212, Oct. 2000, to be published in NIMPR.

[7] M. Bassetti and G. Erskine, CERN ISR TH/80-06 (1980).

[8] H. Fukuma *et al.*, Proc. EPAC2000 (Vienna), p. 1124.